ORIGINAL ARTICLE

A Comparative Study of Optical System to Improve Image Quality of Smartphone-based Ophthalmoscope

Harnani Hassan[1], Nik Amir Afif Nik Ahmad Rushdi[1], Sukreen Hana Herman[1], Sijung Hu[3], and Zulfakri Mohamad[1,2]

[1] School of Electrical Engineering, College of Engineering, Universiti Teknologi MARA, 40450 Shah Alam, Selangor, Malaysia
[2] Research Center for Neutrino Science, Tohoku University, Sendai, 980-8578, Japan
[3] Photonics Engineering and Health Technology Group, Loughborough University, LE11 3TU, UK

ABSTRACT

Introduction: This paper presents a comparative study of an optical system of a smartphone-based ophthalmoscope to improve the image quality of retinal imaging photoplethysmography (iPPG). **Methods:** This study has developed two optical systems using WinLens 3D software. Design I employed the combination of best forms and aspheric lenses while Design II was formed by combining achromatic and 20D lenses. These optical systems were developed to observe: (i) illuminating path when the rays travel from light source to the retina and (ii) imaging path when the ray travel from the retina back to the image sensor of the smartphone camera. **Results:** The outcomes of the observations were presented as the image metric quantities: (i) spot diagram, (ii) transverse ray aberration, and (iii) 3D wavefront plot that represent the image quality of the optical system. Also, the illumination and imaging paths were demonstrated with different focal lengths and similar lens selections to observe the image quality. **Conclusion:** The results showed that Design II has better performance than Design I. The simulation results have provided enough information to verify the performance of the optical design.

Keywords: Smartphone-based ophthalmoscope, Spot diagram, Transverse ray aberration, 3D wavefront plot

Corresponding Author:
Harnani Hassan,
Email: harnani@uitm.edu.my
Tel: +603-55211889

INTRODUCTION

The World Report on Vision in 2019 reveals that there are at least 2.2 billion people are diagnosed with vision deficiency or blindness (1)(2). The vision deficiency and impairment are preventable with current technology, good treatment, comprehension of disease, and health care treatment (2)(3). Due to this reason, and the increase of the aging population, there is a high demand for diagnosing and monitoring devices to improve the eye health care system and treatment. Patients with eye disease need regular screening and monitoring involve tissue layer examination through the eye pupil (ophthalmoscopy), and also visualization of abnormalities regarding the eye diseases(4). The ophthalmoscopy technique was established in 1851 by Hermann von Helmholtz (5). The conventional ophthalmoscope invention possessed three important elements that affect the image quality: (i) a source of illumination, (ii) a way of projecting the light into the eye, and (iii) an optical component arrangement. These elements have become fundamental to modern ophthalmoscope designs today. The technique used fundus photograph to identify abnormalities on the eye tissue due to eye diseases (4).

Over the years, the screening, diagnostic, and treatment techniques of eye disease have evolved tremendously with great achievement. A gold-standard modality such as Optical Coherent Tomography (OCT) is equipped with high-tech features to visualize, identify abnormalities, and effectively monitor the eye health status (6) (7). However, the modality is bulky, table-mounted which is not suitable for home-based assessment, emergency room, and unportable. Also, it requires a skilled practitioner to operate and maintain the modality performance. The smartphone-based ophthalmoscope has recently been designed as an alternative for these shortcomings (8) (9). Despite simple illumination design, minimal settings, and portability, the smartphone-based ophthalmoscope has proven its

capability to assess eye health status by maintaining fundamental design to its simple system (10). Today, a rapid technology of smartphone design with a high-resolution megapixel (MP) camera, compact design, and high frame rate (≥25 frames per second) has improved its capability to capture an image or to record a video (11)(12). These features have improved the capability and reliability of smartphones as retinal imaging devices in the future (13)(14).

This paper presents, a comparative study of two optical systems that were designed for smartphone-based ophthalmoscopes using WinLens 3D software (15) (16). The study was conducted to compare the image quality due to different focal lengths with similar lens arrangements. The optical systems were designed by using three lenses and a single prism to reduce the complexity and cost. In the lens arrangement, a single prism was used to balance the tolerance between the illumination path and the imaging path. The optical systems were demonstrated to observe: (i) an illumination path, which illustrates rays travel from the light source to the retina, and (ii) an imaging path to predicting the behavior of the rays' travel from the retina to the image sensor of the smartphone camera. The quality of the produced image was evaluated regarding (i) symmetrical spot diagram, (ii) transverse ray aberration from illumination path, and (iii) 3D wavefront plot generated from the imaging path (15). Also, the simulations on the effect of lens distance in lens arrangement were demonstrated in both designs. The initial distance of lens arrangement was demonstrated with ±20% and ±40% distances to evaluate the image quality.

MATERIALS AND METHODS

The development of optical design involves the understanding of the principle of ophthalmoscope (17): (i) direct ophthalmoscope, and (ii) indirect ophthalmoscope.

Direct Ophthalmoscope

The direct ophthalmoscope is commonly used to visualize the retina and optic disc. To demonstrate a direct ophthalmoscope, the lens power is adjusted to visualize the patient's retina from 8 cm to 50 cm to the observer's point with approximately 15 times magnification (18).

Indirect Ophthalmoscope

The indirect ophthalmoscope requires condensing lens such as aspheric lens with 2 to 5 times magnifications to reduce distortion and gain a larger field of view (FOV). The produce image is real, reversed or inverted that useful for peripheral view. To demonstrate an indirect ophthalmoscope, a higher intensity of the light source is needed, a large aspheric lens and head-mounted optical system are used where the lens is held in front of the dilated patient's eye (18).

Design and Simulation

In this work, two optical systems were designed using WinLens 3D, an open-source software (16) to observe the ray tracing and quality of the produced image based on indirect ophthalmoscope principle. For both designs, the ray tracing was divided into two paths: (i) illumination paths, and (ii) imaging paths. The outcomes of ray tracing can be interpreted in terms of spot diagram, transverse ray aberration, and 3D wavefront plot (15).

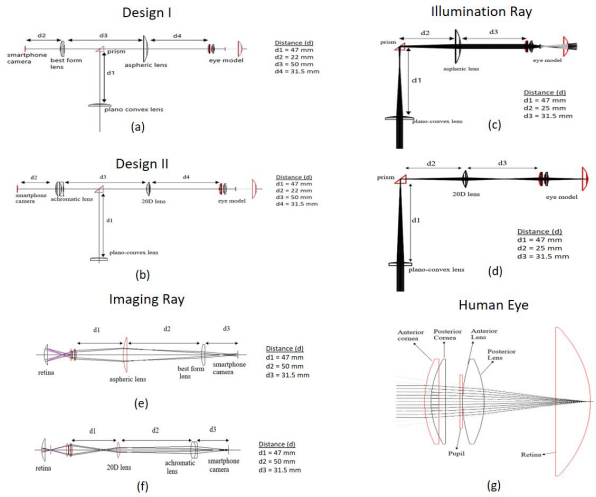

Fig 1 : (a) An Optical system of Design I, **(b)** An optical system of Design II, **(c)** The illumination ray tracing and description of Design I, **(d)** The illumination ray tracing, description of Design II, **(e)** The imaging ray tracing of Design I, **(f)** The imaging ray tracing of Design II, and **(g)** The human eye optical model.

Optical arrangement for smartphone-based ophthalmoscope

To design an established with good performance of the optical system: (i) the lens arrangement, (ii) selection of lens, (iii) optimal design with minimal complexity of lens arrangement need to be considered (15)(19). The lens arrangement of both designs is illustrated in Fig. 1a and 1b. The selection of lenses for each design was tabulated in Table I.

Optical System Design I

For each design, three lenses were used and arranged with similar distances. Ideally, to produce a good optical system of the ophthalmoscope, a high number of lenses is required to produce high-quality images (10). However, in this study, only the fundamental lenses and components of a fundus camera were used to reduce lens arrangement complexity, and prototyping cost.

Optical System Design II

The lens radius and focal length of both designs

Table I : Specification of Lenses for Design I and Design II

Design	Lenses	Radius of curvature (mm)	Glass type	Focal length (mm)	Conic constant
Design I	Plano-Convex Lens	-19.667	N-BK7	37.960	0.000
	Aspheric lens	-31.513	S-LAH64	40.000	-0.641
	Best Form Lens	S1=24.317 S2=-134.325	N-BK7	25.400	0.000
Design II	Plano-Convex Lens	-25.858	N-BK7	50.030	0.000
	20D lens	S1=11.640 S2=-9.480	H-K51	10.360	S1= -1.070 S2=-9.240
	Achromatic lens	S1=13.973 S2=-9.339 S3=-76.140	S-BAH11 N-SF10	19.950	0.000

were slightly different due to the different lens selections. However, the lens arrangements were similar for both designs.

Illumination path from the light source to the retina

An illumination path is essential to observe the ray of light source that travels passes the lenses into the retina. The observation is demonstrated to predict and produce a sharp image at the monitor display (20). A typical fundus camera optical system was designed with a light source that was allocated at the bottom of the design to project a ray of light. The projected light was passed through the lenses at the 90˚ vertical axis which allowed the ray to travel in parallel. Each design possesses a plano-convex lens at the bottom and a similar distance between lenses however, the designs have a different radius and focal length arrangement. As the ray passes through the prism, the ray of light traveled 90 vertically and continued to the condensing lens (20D and aspheric lens) that was used to focus the rays. Finally, the ray passes through the human eyes and reaches the retina. The design of the illumination path for both designs is illustrated in Fig. 1c and 1d.

Imaging path from the retina to the image sensor of smartphone camera

An imaging path is used to observe the behavior of the ray's travel from the retina to the image sensor of the smartphone camera. The imaging path started from the retina through the eye lenses and the condensing lens (aspheric lens and 20D lens). As the ray continued to travel and pass through the next lenses (best form lens and achromatic lens) before it reached the smartphone image sensor. These lenses were used to minimize the aberration value of the design. In Design I, the best form lens was used while Design II possesses an achromatic lens in the lens arrangement. The imaging path for both designs is illustrated as in Fig. 1e and 1f.

Table II : Specification of Eye Model

Surface type	Radius of curvature	Thickness	Refractive index for glass	Diameter	Conic constant
Anterior cornea	11.700	-0.550	1.376	23.000	-0.260
Posterior cornea	9.800	3.000	1.337	19.200	0.000
Pupil	0.000	0.000	1.337	0.000	0.000
Anterior lens	15.000	2.160	1.371	30.000	-3.132
Posterior lens	-11.000	20.600	1.371	21.500	-1.000
Retina	12.000	N/A	1.336	20.000	0.000

Optical model of human eyes

In this work, modeling the human eyes optical system is required to produce the imaging ray from the retina back to the image sensor of the smartphone camera. The human eye was modeled using a similar approach in with surface types, (i) anterior cornea, (ii) posterior cornea, (iii) anterior lens, (iv) posterior lens, and (v) retina (21)(22). The eye model is illustrated as Fig.1g and the parameters are tabulated in Table II.

Simulation of various distance in the lens arrangement

In this work, the distance of lens arrangement of both designs followed the standard fundus camera (23). Also, the simulation of distance lens arrangement was conducted to investigate the influence of lens distance on image quality. The simulation was demonstrated by decreasing and increasing the implemented lens arrangement of Design I and Design II in Fig. 1a and 1b by ±20% and 40%. The various distance setting for Design I and Design II is tabulated in Table III.

RESULTS

The WinLens 3D software can be used to determine and observe a variety of image quality metrics. However, in this work, there are three image quality metrics were considered: (i) spot diagram, (ii) transverse ray aberration, and (iii) 3D wavefront plot. These metric qualities are chosen based on the application of the optical system (15).

Spot diagram

The spot diagram appeared as a spot when it traces a large number of a ray of light travel through the lenses from point of the source. The spot diagram plotted the location of rays when they traverse with the image plane (24). The observation shows at 0.0mm the spot diagram of Design II in Fig. 2b has better symmetrical where most of the ray convergence to the center.

Transverse ray aberration

The demonstration of transverse ray aberration in Fig. 2c and 2d showed that the line graph at (c) of Design II was almost approaching the horizontal line which indicates the design has minimum aberration. While Design I showed the line graph at (c) was about 60% more to approach the horizontal line which also indicates the numerous aberrations in the optical system.

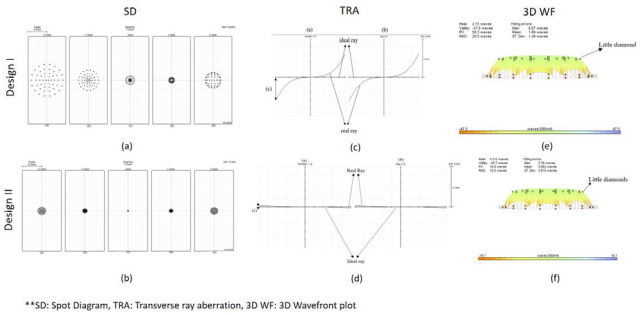

Fig 2 : (a) Spot diagram of Design I : (a) focus shift by -2.0mm, (b) focus shift by -1.0mm, (c) focus shit by 0.00mm, (d) focus shit by 1.0mm, and (e) focus shift by 0.02mm, **(b)** Spot diagram of Design II : (a) focus shift by -2.0mm, (b) focus shift by -1.0mm, (c) focus shit by 0.00mm, (d) focus shit by 1.0mm and (e) focus shift by 0.02mm, **(c)** Transverse ray aberration of Design I, **(d)** Transverse ray aberration of Design II, (d) The wavefront surface of Design I with PV = 50.3 waves and RMS =28.5 waves and **(e)** The wavefront surface of Design II with PV = 16.9 waves and RMS 10.0 waves.

Table III : Distance Setting of Lens Arrangement for Design I and Design II

Design	Distance Setting	-40% (mm)	-20% (mm)	+20% (mm)	+40% (mm)
Design I	Distance between plano-convex lens and prism	28.20	37.50	58.75	65.80
	Distance between a prism and aspheric lens	15.00	20.00	30.00	35.00
	Distance between an aspheric lens and eye model,	18.90	24.70	38.30	44.10
	Distance between the aspheric lens with best form lens	30.00	40.00	60.00	70.00
Design II	Distance between plano-convex lens and prism	28.20	37.50	58.70	65.80
	Distance between prism and 20D lens	15.00	20.00	30.00	35.00
	Distance bewteen 20D and eye model,	18.90	24.70	38.30	44.10
	Distance between an aspheric lens with best form lens	30.00	40.00	60.00	70.00

3D wavefront plot

The 3D wavefront plot in Fig. 2e and 2f showed that both designs have produced a smooth wavefront where rays reached the surface by observing the 'little diamonds'. This means that the light that was successfully traveled from the retina and reached the image sensor of the smartphone camera. The Peak-to-Valley (PV) error values produced from both designs were considered as fair optical quality because they produced above 1/8 wave. The produced wave was ≤ 70 nm of the 560 nm for a warm white light source that is commonly used for eye modality.

Effect of lens distance on image quality

In this work, the various lenses distance was demonstrated to investigate the effect of these distances on image quality. The results of Design I and Design II were illustrated in Fig. 3 showed Design II is better than Design I according to Fig. 3e and 3g.

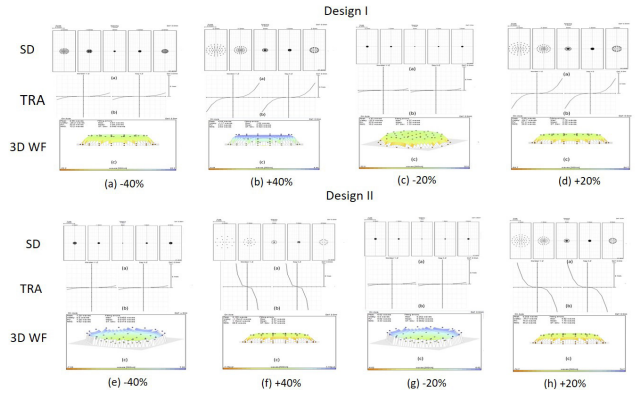

Fig 3 : Spot diagram (SD), Transverse ray aberration (TRA), and 3D Wavefront plot (3D WF) of Design I with various lens distance at (a)-40%, (b)+40%, (c)-20% and (d)+20% and Design II with various lens distance at (e)-40%, (f)+40%, (g)-20% and (h)+20%.

DISCUSSION

Spot Diagram

To produce a good and sharp image quality, the ray must fall to the image plane with a smaller spot (19)(24). By observation, the spot diagram of Design II in Fig. 2b at focus 0.0mm produced a smaller spot diagram than Design I in Fig. 2a at focus 0.0 mm. The observation indicates that Design II produced a sharper image compared to Design I. The spot diagram produced in Design I implies that the design has a spherical aberration error.

Transverse ray aberration

Transverse ray aberration was demonstrated to map the image positions of rays in each fan that related to the chief ray versus the position of the rays at the entrance pupil (25). The ray aberration curves trace fans of rays were categorized in two orthogonal directions (i) meridian Y-Z axis at (a), and (ii) sagittal X-Z axis at (b). The function of transverse ray aberration for this application is to identify the ray position image in a fan and the differences in the intercept of an actual ray concerning the ideal image point (26). A perfect optical system produces a straight line along the horizontal axis in both the meridian (a) and the sagittal axis (b) that represent an ideal ray. Therefore, the more closer ray is produced to the ideal ray, it indicates that the aberration of the optical system is minimized.

3D wavefront plot

The wavefront plot is calculated by tracing concentric rings of rays from each object point through the lens aperture. The ray location in the aperture is shown by the 'little diamonds'. In 3D wavefront plot, the measurement was based on: (i) PV and RMS, (ii) peak, and (iii) valley. The 'peak' can be defined as the most positive Optical Path Difference (OPD) value from any of the rays and the 'valley' is defined to be the most negative OPD value from any of the rays. The Peak-to-Valley (PV) is obtained from the differences between 'peak' and 'valley' values. The Root Mean Square (RMS) of OPD values from all rays that have been traced from the selected object point (27). The measurement of RMS represents more than an averaged value over the entire set. The measured RMS value could be small, even though the PV value is large. The PV value is more likely referred to than the RMS value to evaluate the image quality. However, the RMS value is a better method to measure the feat of an optic than PV and neither one of these parameters are useful to calculate the optics performance. The waves characteristic and optical quality that relates to PV error where below and 1/3 is classified as very poor and poor, and 1/8 and above is classified as minimally good and better. The optical system with PV error that produces 1/8 waves and above value are considered to possess good optical quality. For instance, at 250 nm the wave is about wave if blue-green light is considered as reference (500 nm).

CONCLUSION

This work has presented a comparative study of the optical system to improve image quality for retinal imaging photoplethysmography (iPPG). Two illumination designs were proposed and the effect of lens distance on the image quality was also investigated. The image quality metrics produced from the illumination path and imaging path were considered in this work. The correct selection of lenses and accurate lens distance in the lens arrangement was also crucial to optimize the optical system performance. From observation results and performance of both designs, it is discovered that Design II has produced a better result than Design I in terms of spot diagram, transverse ray aberration,

Table IV : Effects of Lenses Distance on Image Quality Metrics

Design	Image quality metrics	+40%	-40%	+20%	-20%	Comments
Design I	Spot diagram	x	√	x	√	At +40%, the ray started sparse
	Transverse aberration	x	√	x	√	At -40% and -20%, the graph line was closer to the horizontal axis
	3D waveform plot	-	-	x	√	There was no significant different at ±40%, where some of the ray has not reached target surface. But more ray reached target surface at -20%.
Design II	Spot diagram	x	√	x	√	At -20%, the spot diagram produced was sharp
	Transverse aberration	x	√	x	√	The aberrations at -40% and -20% were better, the graph line produced was closer to the horizontal axis.
	3D waveform plot	-	-	√	√	At ±40%, the ray was not evenly sparse and some failed to reach target surface. At ±20%, the 3D wavefront plot showed quite good performance as most of the rays reached the targeted surface.

**Indicator: '√' – Better, 'x' – Poor, '- '- No different

and 3D wavefront plot. The demonstration on lens distance has concluded that the lens distance modification has influenced the produced image quality. In this work, a basic version of WinLens 3D open-source software is used to design and demonstrate the optical systems.However, the image metric quality is accessible and can be used to provide enough information to verify optical system performance. For future work, the image quality can be improved by using a full license of WinLens 3D where more performance aspects can be accessed and demonstrated.

ACKNOWLEDGEMENT

This work was financially supported by Universiti Teknologi MARA, Shah Alam, Malaysia.

REFERENCES

1. McCormick I, Mactaggart I, Resnikoff S, Muirhead D, Murthy G V., Silva JC, et al. Eye health indicators for universal health coverage: Results of a global expert prioritisation process. Br J Ophthalmol. 2021;1–9. Available from: http://dx.doi.org/10.1136/bjophthalmol-2020-318481 [Accessed 20th November 2020]
2. Flaxman SR, Bourne RRA, Resnikoff S, Ackland P, Braithwaite T, Cicinelli M V., et al. Global causes of blindness and distance vision impairment 1990–2020: a systematic review and meta-analysis. Lancet Glob Heal. 2017;5(12):e1221–34. Available from: https://doi.org/10.1016/S2214-109X(17)30393-5 [Accessed 12th November 2020]
3. Furtado JM, Reis TF, Eckert KA, Lansingh VC. 2020 and Now: What Has Been Accomplished in Blindness Prevention and What Is Next? Arq Bras Oftalmol. 2020;83(5):V–IX. Available from: https://doi.org/10.5935/0004-2749.20200101 [Accessed 4th November 2020]
4. Chew FLM, Salowi MA, Mustari Z, Husni MA, Hussein E, Adnan TH, et al. Estimates of visual impairment and its causes from the national eye survey in Malaysia (NESII). PLoS One. 2018;13(6):1–11. Available from: https://doi.org/10.1371/journal.pone.0198799 [Accessed 2nd November 2020]
5. Sherman SE. The history of the ophthalmoscope. 1989;221–2. Available from: https://doi.org/10.1007/BF00163473 [Accessed 4th November 2020]
6. Lai TYY. Ocular imaging at the cutting-edge. Eye. 2021;35(1):1–3. Available from: http://dx.doi.org/10.1038/s41433-020-01268-1 [Accessed 30th October 2020]
7. Yasin Alibhai A, Moult EM, Shahzad R, Rebhun CB, Moreira-Neto C, McGowan M, et al. Quantifying Microvascular Changes Using OCT Angiography in Diabetic Eyes without Clinical Evidence of Retinopathy. Ophthalmol Retin. 2018 May;2(5):418–27. Available from: https://doi.org/10.1016/j.oret.2017.09.011 [Accessed 25th October 2020]
8. Rajalakshmi R, Subashini R, Anjana RM, Mohan V. Automated diabetic retinopathy detection in smartphone-based fundus photography using artificial intelligence. Eye. 2018;32(6):1138–44. Available from: http://dx.doi.org/10.1038/s41433-018-0064-9 [Accessed 15th October 2020]
9. Mamtora S, Sandinha MT, Ajith A, Song A, Steel DHW. Smart phone ophthalmoscopy: a potential replacement for the direct ophthalmoscope. Eye.

2018;32(11):1766–71. Available from: http://dx.doi.org/10.1038/s41433-018-0177-1 [Accessed 15th December 2020]
10. Patel TP, Kim TN, Yu G, Dedania VS, Lieu P, Qian CX, et al. Smartphone-based, rapid, wide-field fundus photography for diagnosis of pediatric retinal diseases. Transl Vis Sci Technol. 2019;8(3). Available from: https://doi.org/10.1167/tvst.8.3.29 [Accessed 17th December 2020]
11. Wintergerst MWM, Jansen LG, Holz FG, Finger RP. A novel device for smartphone-based fundus imaging and documentation in clinical practice: Comparative image analysis study. JMIR mHealth uHealth. 2020;8(7):1–11. Available from: https://doi.org/10.2196/17480 [Accessed 20th December 2020]
12. Tran, K., Mendel, T. A., Holbrook, K. L., & Yates, P. A. (2012). Construction of an inexpensive, hand-held fundus camera through modification of a consumer "point-and-shoot" camera. Investigative ophthalmology & visual science, 53(12), 7600–7607. Available from: https://doi.org/10.1167/iovs.12-10449 [Accessed 28th December 2020]
13. Sosale B, Aravind SR, Murthy H, Narayana S, Sharma U, Gowda SG V, et al. Simple, Mobile-based Artificial Intelligence Algorithm in the detection of Diabetic Retinopathy (SMART) study. BMJ Open Diabetes Res & Care ;8(1):e000892. Available from: http://drc.bmj.com/content/8/1/e000892.abstract [Accessed 5th January 2021]
14. Pieczynski J, Kuklo P, Grzybowski A. The Role of Telemedicine, In-Home Testing and Artificial Intelligence to Alleviate an Increasingly Burdened Healthcare System: Diabetic Retinopathy. Ophthalmol Ther. 2021;10(3):445–64. Available from: https://doi.org/10.1007/s40123-021-00353-2 [Accessed 12th January 2021]
15. Qioptiq. WinLens. 2013. Available from: https://www.qioptiq-shop.com/en/Optics-Software/Winlens-Optical-Design-Software/Free-Winlens-Basic/ [Accessed 15th October 2020]
16. Gerhard C, Adams G. Easy-to-use software tools for teaching the basics, design and applications of optical components and systems. Educ Train Opt Photonics ETOP 2015. 2015;9793(October 2015):97930N. Available from: https://doi.org/10.1117/12.2223079 [Accessed 12th January 2021]
17. Iqbal U. Smartphone fundus photography: a narrative review. Int J Retin Vitr. 2021;7(1):1–12. Available from: https://doi.org/10.1186/s40942-021-00313-9 [Accessed 20th January 2021]
18. Timberlake G KM. The Direct Ophthalmoscope How it Works and How to Use It. 2008. 2008. p. 1–39. Available from: http://web.media.mit.edu/~raskar/Eye/TheDirectOphthalmoscope.pdf%5Cnpapers3://publication/uuid/DEC95CF9-781B-46D3-9772-9800B907AB8D [Accessed 15th January 2021]
19. Thuniss T, Adams G, Gerhard C. Optical System design. Opt Photonik. 2009;4(2):30–3. Available from: https://doi.org/10.1002/opph.201190022 [Accessed 23th January 2021]
20. Mueller P, Lehmann M, Braun A. Optical quality metrics for image restoration. In: ProcSPIE. 2019. Available from: https://doi.org/10.1117/12.2528100 [Accessed 23th January 2021]
21. World scientific. Basic Anatomy of the Eye , Adnexa. 2021;1–31. Available from: https://doi.org/10.1142/9789813275607_0001 [Accessed 23th January 2021]
22. Melo DS De. completo Design of a Retinal Image Acquisition Device for Mo- bile Diabetic Retinopathy Assessment. 2017;1–41. Available from: http://hdl.handle.net/10362/27916 [Accessed 23th November 2020]
23. Kim TN, Myers F, Reber C, Loury PJ, Loumou P, Webster D, et al. A Smartphone-Based Tool for Rapid, Portable, and Automated Wide-Field Retinal Imaging. Transl Vis Sci Technol . 2018 Oct 1;7(5):21. Available from: https://pubmed.ncbi.nlm.nih.gov/30280006 [Accessed 17th November 2020]
24. Herzberger M. Analysis of Spot Diagrams$\ast$. J Opt Soc Am. 1957 Jul;47(7):584–94. Available from: http://www.osapublishing.org/abstract.cfm?URI=josa-47-7-584 [Accessed 10th November 2020]
25. Dereniak EL, Dereniak TD. Geometrical and Trigonometric Optics. Cambridge: Cambridge University Press; 2008. Available from: https://www.cambridge.org/core/books/geometrical-and-trigonometric-optics/41792CC511FABC71B070C0747CBB42D0 [Accessed 10th February 2021]
26. EDMUND. Comparison of Optical Aberrations. Available from: https://www.edmundoptics.com/knowledge-center/application-notes/optics/comparison-of-optical-aberrations/ [Accessed 5th February 2021]
27. Wyant JC, Creath K. Basic wavefront aberration theory. Vol. Xl, Applied Optics and Optical Engineering. 1992. 1–53 p. Available from: http://fp.optics.arizona.edu/OPTI471b/Reading/Lab6/Chapter3%7B_%7DBasicAberrationsandOpticalTesting.pdf%5Cnhttp://fp.optics.arizona.edu/OPTI471b/Reading/Lab6/Chapter3_BasicAberrationsandOpticalTesting.pdf [Accessed 18th February 2021]